Supporting Information

Dugas-Ford et al. 10.1073/pnas.1204773109

SI Text

While this report was under review, Suzuki et al. (1) published a short article in the April 2012 issue of *Developmental Cell* titled "The Temporal Sequence of the Mammalian Neocortical Neurogenetic Program Drives Mediolateral Pattern in the Chick Pallium." Based on the gene expression patterns of neocortical layer 2/3 (*CUX2*, *SATB2*, *MEF2C*, *FOXP1*) and layer 5/6 (*CTIP2*, *ER81*, *FEZF2*) molecular markers in chick dorsal telencephalon, the authors conclude that the chick parahippocampal area contains cells that are homologous to deep-layer neocortical neurons, and the mesopallium shares a homology with the upper layers. Here we describe why these conclusions, particularly those regarding the layer 5 neurons, are deeply problematic.

Neither connectional nor molecular data support the hypothesis of a homology between neurons in the chick parahippocampal area and neurons in layer 5 of neocortex. Atoji and Wild (2) examined the organization of the pigeon medial pallium with a variety of tract-tracing methods and concluded that the territory Suzuki et al. (1) describe as "deep neocortical layers" is comparable to Ammon's horn and the subiculum; they refer to this region as the dorsomedial hippocampal formation (DM). Just medial to DM lies what Atoji and Wild (2) called the triangular region and the V-shaped layer, with the latter described as similar in its connections to the dentate gyrus of the mammalian hippocampus.

We found that molecular data support Atoji and Wild's (2) conclusions. We examined the gene expression of layer 5 markers *Er81*, *Fezf2*, and *Pcp4* in adult ferret, mouse, and chicken brains (Fig. S7). We found that, in addition to their neocortical layer 5 expression, *Er81* and *Fezf2* are also dense in the subiculum of both mammalian species. By contrast, *Pcp4* gene expression, although strong in the deep neocortical layers, only identified scattered cells in the subiculum. These *Pcp4* neurons appear from their location to correspond to the small population of subicular neurons that project to thalamus (3). We found very similar expression patterns in the chick parahippocampal area. Both *ER81* and *FEZF2* are expressed in DM, with *ER81* labeling being particularly heavy, but only a few *PCP4*-rich cells were detected. Finally, the *ER81*-positive DM territory immediately adjoins the triangular region and V-shaped layer, which express the mouse dentate gyrus marker *PROX1* (4). These molecular data provide strong support for the long-held view (5) that the chick medial pallium is homologous to the mammalian hippocampal formation. More specifically, these data support the connectional hypothesis that the DM region represents part of the hippocampal formation and contradict Suzuki et al.'s (1) claim of homology with deep layers of neocortex.

Whether there are cells in the chick dorsal telencephalon that are homologous to neurons in layers 2 and 3 (L2/3) of the neocortex is an important question that we did not address in our report, in part because the identification of L2/3 molecular markers has proven challenging; many candidates are not specific to L2/3 or show restricted expression only within particular cortical areas. For example, *CUX2* expression in primates is restricted to L2/3 in V2, but is expressed in layers 2–4 in area V1 (6). A closely related molecular marker, *Cux1*, identifies layers 2–4 in primary sensory areas of ferret and mouse, but shifts this layer selectivity in other cortical areas (7, 8).

Two upper-layer markers used by Suzuki et al. (1), *Mef2c* and *Satb2*, are particularly problematic. These markers are expressed in the upper layers during neocortical development, and *Satb2* has been implicated in the differentiation of the callosal projection neurons in layers 2–5 (9–12). We found, however, that these genes do not specifically identify L2/3 in the adult mouse, and are instead expressed strongly in layers 2 through 6 (Fig. S8 *A* and *B*). These genes are also widely expressed in the chicken dorsal telencephalon (Fig. S8 *C* and *D*). Overall, these data are uninformative with regards to L2/3 cell-type homology across birds and mammals, so there is no secure molecular evidence to support Suzuki et al.'s (1) claim that the mesopallium shares a homology with the upper layers of neocortex.

To identify cells that are homologous to neocortical L2/3 neurons in nonmammalian amniotes, we recommend a strategy similar to the approach used in our study. First, it is necessary to show that candidate L2/3 markers are selectively enriched in L2/3 across much or all of the neocortex and that they are stable L2/3 markers in distantly related mammalian species. Second, the expression of these L2/3 markers should be studied in more than one nonmammalian species. A particular requirement for a conclusion about homology by descent is that these cell types be demonstrated in the cortex of at least one reptile. Finally, in all animals, the gene expression patterns should identify territories with connections similar to those of neocortical L2/3. Once these criteria are met, a conclusion that there is a L2/3 cell type conserved across the amniotes would be warranted; for now, this remains an open question in evolutionary neurobiology.

SI Materials and Methods

Animals and Tissue. Fertilized White Leghorn chicken eggs (*Gallus gallus domesticus*) were purchased from Phil's Fresh Eggs and incubated in a humidified forced-air chamber (Humidaire; G.Q.F. Manufacturing Co.). On the day of hatching (P0), chicks were moved to a universal box brooder (McMurray Hatchery). Chicks were harvested at P0 or between 2 and 3 wk of age (P14, P15, P19). The University of Chicago Transgenic Mouse Core supplied the adult mice. Adult ferrets (*Mustela putorius furo*) were obtained from Marshall Farms. Adult turtles (*Trachemys scripta*) were purchased from Kons Scientific and generously donated by Jay Goldberg (University of Chicago, Chicago). Dan Margoliash and his laboratory (University of Chicago, Chicago) supplied the adult male zebra finches (*Taeniopygia guttata*). All animals were deeply anesthetized with sodium pentobarbital (120 mg/kg) and perfused through the heart with 4% paraformaldehyde in 0.1 M PBS [paraformaldehyde (PFA)-PBS (pH 7.4)]. Brains were removed and immersed in PFA-PBS overnight and placed in a 30% sucrose/PFA-PBS solution for cryoprotection. Sections were cut at 32–36 μm on a sledge microtome. Sections were mounted on Fisherbrand Superfrost Plus slides and dried thoroughly. All animal procedures were reviewed and approved by the Institutional Animal Care and Use Committee of the University of Chicago.

cDNA Cloning. cDNA fragments isolated for this report were generated by PCR on cDNA synthesized from total brain RNA of chicken embryos and adult mice, ferrets, turtles, and zebra finches. Primers were designed with MacVector software applied to chicken, mouse, and dog genomic and EST sequences or with the CODEHOP program drawing on vertebrate protein databases (13). *cPCP4* fragment was isolated from chicken genomic DNA. The PCR fragments were subcloned in pCRII-TOPO vector (Invitrogen).

cCACNA1H forward: 5′-CCCATCCAGAACCATAACCCTTG-3′; reverse: 5′-CGAAAACCAAATGCCACCAAC-3′
cEAG2 forward: 5′-CATAGCACCAACCACTGATGGG-3′; reverse: 5′-AGGAATAGGGTAGAAGGGATGCC-3′
cFEZF2 forward: 5′-TTCAACTACCTGGATGCCGCCTAC-3′; reverse: 5′-AAATCCTTTGCCGCAAGTGAC-3′

cKCNN2 (GenBank AF079372) forward: 5′-ATGCCTTATCAGCCTCTCCACG-3′; reverse: 5′-GATGTTTTGAGTCTTTGCCAGGTC-3′
cMEF2C forward: 5′-CAATGCCATCAGTGAATCAGAGG-3′; reverse: 5′-ATCTTCTCGGTCGCTCCCATCG-3′
cPCP4 forward: 5′-ATGTGCTGAAAGGGATGAGGCAGG-3′; reverse: 5′- TGACTGGATGGAGAGTGAACGGAG-3′
cSATB2 (GenBank HM776640) forward: 5′-CCTGCGTAAAGAAGAAGACCCC-3′; reverse: 5′-CTCTGCCACATCAACCACTGTTC-3′
cSULF2 forward: 5′-CGAGAAACATCACCAAGCGG-3′; reverse: 5′-AGGTCCAGCAGTTGAGGCAGTTAG-3′
cTMEM200A forward: 5′-AACTGACACCGATGAATCCTGC-3′; reverse: 5′-CAACTCGCTGAGCACTGATAATG-3′
cVGLUT2 (GenBank JF320001) forward: 5′-TCAATAACAGCACCATACACCGAG-3′; reverse: 5′-TCCGCTAAAGCCTACAGCAAGC-3′
fTMEM200A forward: 5′-GTTGTTCGTGGCAAAATCCG-3′; reverse: 5′-GCAATGTAAAAGCACTGATGGACG-3′
fWHRN forward: 5′-TTCACGCACTGCCTCAACGCCTAC-3′; reverse: 5′-TGGCGATCCACTTGGTCTC-3′
mSatb2 (GenBank BC138626) forward: 5′-AAGAGTGGAGCGAGAGAACCTTTC-3′; reverse: 5′-CAAACAGGGCTTGAGACACCTTG-3′
mTmem200a (GenBank AK173299) forward: 5′-TGGGAGTGCTGGTGTCCATCATAG-3′; reverse: 5′-TAGTTTTGAGGTTGTCTGCGACC-3′
mWhrn (GenBank AY739116) forward: 5′-AGTTCACTCACTGCCTCAACGC-3′; reverse: 5′-TTCTGTGTGGTCCCCTGGAAAC-3′
tEAG2 forward: 5′-CTTAGGGAAAGGTGATGTGTTTGG-3′; reverse: 5′-GATGTCTGGATGGGGGTRATCTG-3′
tELAVL4 forward: 5′-TGAGAGACAAAATCACAGGGCAG-3′; reverse: 5′-CATCTGAGTCGGGAGACAAGTTG-3′
tER81 forward: 5′-CCTGTACAACGTGTCCGCCTAYGAYCARAA-3′; reverse: 5′-CACATATCTTTCTCCGGCCACYTTYTGCAT-3′
tGAD1 (GenBank AF043274) forward: 5′-ATTCTCACCTGGAGGGGCTATC-3′; reverse: 5′-TGACGATGCTTCCTGGACATTAG-3′
tRORB forward: 5′-GGAGGAGTCAGCAGAACAAYGC-3′; reverse: 5′-CGGAACCCAAGGCTTTRAAC-3′
tgEAG2 forward: 5′-CTTAGGGAAAGGTGATGTGTTTGG-3′; reverse: 5′-GATGTCTGGATGGGGGTRATCTG-3′
tgER81 forward: 5′-CCTGTACAACGTGTCCGCCTAYGAYCARAA-3′; reverse: 5′-TGCATGTAGGCCATGGTCTCRTCRAA-3′
tgRORB forward: 5′- GGAGGAGTCAGCAGAACAAYGC-3′; reverse: 5′- CGGAACCCAAGGCTTTRAAC-3′

cDNAs for mouse *Er81* and chicken *ER81* and *RORB* were gifts from T. Brown (Groton, CT), T. Jessell (New York, NY), and M. Becker-Andre (Geneva, Switzerland), respectively. cDNAs for mouse *Mef2c* and *Prox1* were gifts of E. Grove (University of Chicago, Chicago). The isolation methods for the other mouse, ferret, and chicken cDNAs used in this study have been reported previously (7, 14). cDNAs generated by the Ragsdale Laboratory are available through Addgene or on request.

In Situ Hybridization. Section in situ hybridization (ISH) was carried out as previously described (7, 15). Slide-mounted sections were postfixed in PFA-PBS for 15 min at room temperature (RT), rinsed 3× for 5 min in PBS, and incubated for 30 min to 1 h in proteinase K solution [1 μg/mL proteinase K in 100 mM Tris·HCl (pH 8.0)/50 mM EDTA (pH 8.0)] at 37 °C. Digested sections were fixed for 15 min in PFA-PBS, rinsed in PBS, and placed in hybridization solution (200 μg/mL heparin/12.5 mg/mL yeast RNA/5× SSC/1% SDS/50% formamide). Slides were incubated for 1 h at 72 °C in hybridization solution. Antisense digoxigenin (DIG)-labeled riboprobes were synthesized from linearized plasmid with bacteriophage polymerases. A total of 0.5–2 μg of labeled RNA was added to the hybridization solution. After overnight incubation at 72 °C, the slides were washed 3× for 45 min in 72 °C Solution X (2× SSC/1% SDS/50% formamide) and rinsed 3× for 15 min in RT 25 mM Tris·HCl (pH 7.5)/0.136 M NaCl/2.68 mM KCl/1% Tween 20 (TBST). Sections were incubated in 10% lamb serum in TBST for 1 h at 4 °C. Riboprobe-mRNA duplexes were detected with Fab fragments coupled to alkaline phosphatase (Roche). The antibody conjugate was preadsorbed with chicken embryo power/1% lamb serum/TBST and added to tissue at a 1:5,000 dilution in TBST/1% lamb serum. The antibody reaction proceeded overnight at 4 °C. The slides were washed 5× for 15 min in TBST and once for 15 min in 100 mM Tris·HCl (pH 9.5)/100 mM NaCl/50 mM $MgCl_2$/1% Tween 20. The antibody-decorated duplexes were detected by phosphatase histochemistry using 5-bromo-4-chloro-3-indolyl phosphate (BCIP) and nitro blue tetrazolium (NBT). After 1–5 d incubation, slides were rinsed, postfixed, and coverslipped with Eukitt mounting medium.

For two-color ISH, DIG- and fluorescein (FL)-labeled riboprobes were incubated in a single overnight hybridization reaction with detection of the hapten-labeled riboprobes carried out sequentially. For light microscopic two-color ISH, the first hapten was demonstrated by antibody–phosphatase reactions using the BCIP/NBT substrates. The first antibody–phosphatase complex was inactivated with two 30-min Solution X washes at 72 °C. The second hapten was detected by antibody–phosphatase labeling with BCIP and tetranitro blue tetrazolium (TNBT). For fluorescent two-color ISH, sections were blocked in TBST/B [20% DIG Block Buffer (Roche) in TBST] for 1 h at RT and incubated for 2 h in anti-DIG peroxidase (Roche) or anti-FL peroxidase (Perkin-Elmer) at a 1:200 dilution in TBST/B. These antibodies were not preadsorbed. Slides were washed 3× in TBST for 15 min, and rinsed twice in 0.1 M Tris·HCl (pH 7.5)/0.15 M NaCl/0.05% Tween 20 (TNT) for 5 min. Slides were next incubated for 1 h in tyramide dyes of Cy3, for DIG detection, or FITC, for FL demonstration (1:50 in 1× Plus Amplification Diluent; Perkin-Elmer). Slides were washed 3× for 15 min in TNT, incubated twice for 15 min in 72 °C detergent mix [1% Nonidet P-40/1% SDS/0.5% deoxycholate/50 mM Tris·HCl (pH 7.5)/1 mM EDTA (pH 8.0)/150 mM NaCl], stripped for 30 min in 72 °C Solution X, and rinsed 3× for 15 min in RT TBST. The slides were blocked in TBST/B before second-color demonstration of the other hapten. After fluorescence processing, the slides were rinsed in PBS and coverslipped in ProLong Gold Antifade Reagent (Invitrogen).

Cytochrome Oxidase. Cytochrome oxidase staining was carried out as previously described (16). A 10-mg diaminobenzidine tetrahydrochloride tablet (Sigma) was sonicated for 30 min in reaction solution [3 mg cytochrome *c* (Sigma)/0.8 g sucrose/0.1 M phosphate buffer (pH 7.4)] and passed through a 0.22-μm filter. Slides were incubated in reaction solution in the dark at 37 °C. The reaction was stopped with several rinses in phosphate buffer. Slides were dried and coverslipped in Eukitt mounting medium.

Photomicroscopy. NBT and TNBT reaction products were studied on an Axioskop 40 microscope with AxioCam digital photography (Zeiss). Fluorescent signals were imaged on a total internal reflection fluorescence live-cell microscope (Olympus). Images were processed with Photoshop CS3 (Adobe) and ImageJ (National Institutes of Health), with global adjustments of hue, saturation, and contrast as needed.

1. Suzuki IK, Kawasaki T, Gojobori T, Hirata T (2012) The temporal sequence of the mammalian neocortical neurogenetic program drives mediolateral pattern in the chick pallium. *Dev Cell* 22:863–870.
2. Atoji Y, Wild JM (2004) Fiber connections of the hippocampal formation and septum and subdivisions of the hippocampal formation in the pigeon as revealed by tract tracing and kainic acid lesions. *J Comp Neurol* 475:426–461.
3. Ishizuka N (2001) Laminar organization of the pyramidal cell layer of the subiculum in the rat. *J Comp Neurol* 435:89–110.
4. Pleasure SJ, Collins AE, Lowenstein DH (2000) Unique expression patterns of cell fate molecules delineate sequential stages of dentate gyrus development. *J Neurosci* 20: 6095–6105.
5. Karten HJ, Hodos W (1967) *A Stereotaxic Atlas of the Brain of the Pigeon (Columba livia)* (Johns Hopkins Univ Press, Baltimore).
6. Bernard A, et al. (2012) Transcriptional architecture of the primate neocortex. *Neuron* 73:1083–1099.
7. Rowell JJ, Mallik AK, Dugas-Ford J, Ragsdale CW (2010) Molecular analysis of neocortical layer structure in the ferret. *J Comp Neurol* 518:3272–3289.
8. Nieto M, et al. (2004) Expression of Cux-1 and Cux-2 in the subventricular zone and upper layers II-IV of the cerebral cortex. *J Comp Neurol* 479:168–180.
9. Leifer D, et al. (1993) MEF2C, a MADS/MEF2-family transcription factor expressed in a laminar distribution in cerebral cortex. *Proc Natl Acad Sci USA* 90: 1546–1550.
10. Britanova O, et al. (2008) Satb2 is a postmitotic determinant for upper-layer neuron specification in the neocortex. *Neuron* 57:378–392.
11. Alcamo EA, et al. (2008) Satb2 regulates callosal projection neuron identity in the developing cerebral cortex. *Neuron* 57:364–377.
12. Tashiro K, et al. (2011) A mammalian conserved element derived from SINE displays enhancer properties recapitulating Satb2 expression in early-born callosal projection neurons. *PLoS ONE* 6:e28497.
13. Rose TM, et al. (1998) Consensus-degenerate hybrid oligonucleotide primers for amplification of distantly related sequences. *Nucleic Acids Res* 26:1628–1635.
14. Sanders TA, Lumsden A, Ragsdale CW (2002) Arcuate plan of chick midbrain development. *J Neurosci* 22:10742–10750.
15. Grove EA, Tole S, Limon J, Yip L, Ragsdale CW (1998) The hem of the embryonic cerebral cortex is defined by the expression of multiple Wnt genes and is compromised in Gli3-deficient mice. *Development* 125:2315–2325.
16. Graybiel AM, Ragsdale CW (1982) Pseudocholinesterase staining in the primary visual pathway of the macaque monkey. *Nature* 299:439–442.

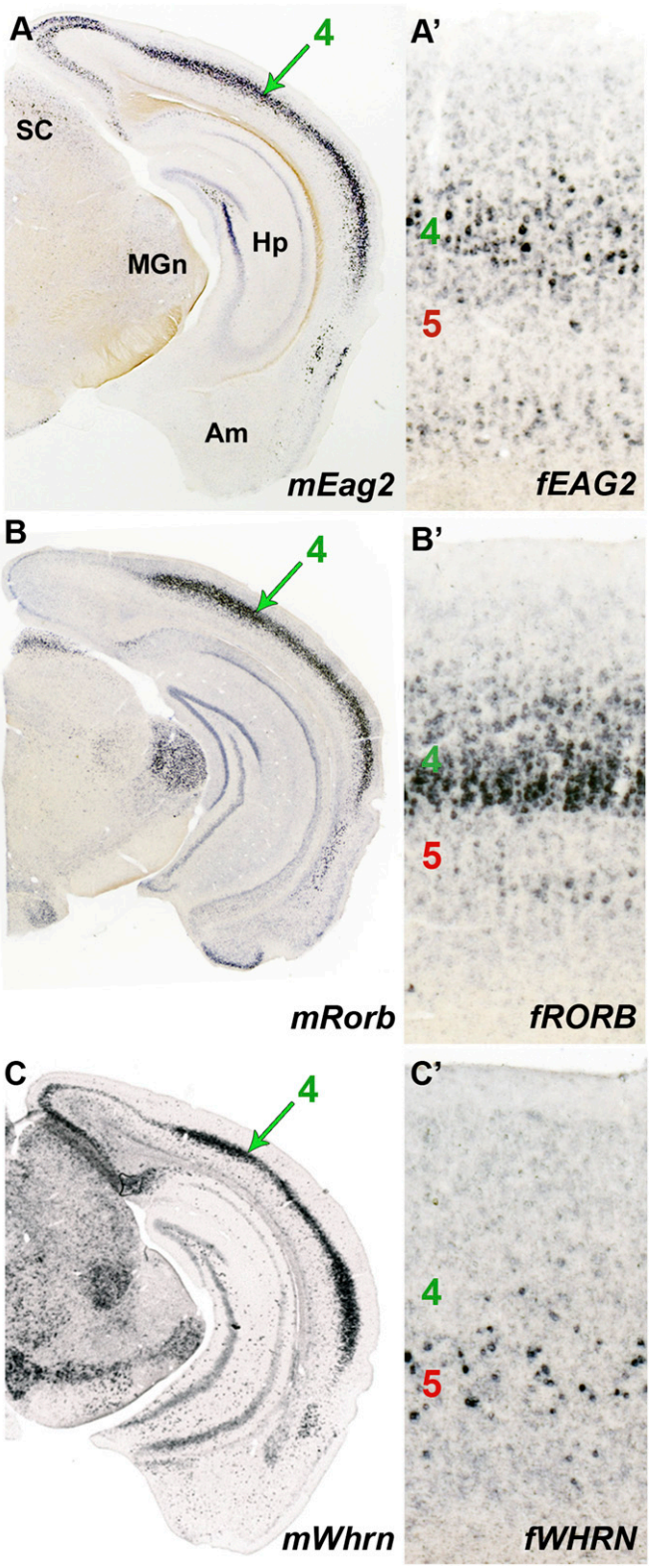

Fig. S1. Molecular characterization of mouse layer 4 markers in mammalian neocortex. (*A*–*C*) ISH experiments demonstrating *Eag2* (*A*), *Rorb* (*B*), and *Whrn* (*C*) gene expression in layer 4 (green arrow) of mouse neocortex. An additional candidate mouse layer 4 marker, *LOC433228I*, has been identified in brain atlas publications from the Allen Institute for Brain Science (1, 2). *LOC433228I* maps to the mouse *Rorb* locus on mouse chromosome 19 and therefore likely corresponds to *Rorb* transcript sequence. (*A*′–*C*′) High-power photomicrographs of area 18 of ferret visual cortex prepared for ISH. *EAG2* (*A*′) and *RORB* (*B*′) are expressed in layer 4, but *WHRN* (*C*′) is not, and so was excluded as a general molecular marker of mammalian layer 4. In both mouse and ferret, scattered cells express *Eag2* and *Rorb* in infragranular cortex (3). 4,5, layers 4 and 5 in ferret neocortex; Am, amygdala; Hp, hippocampal formation; MGn, medial geniculate nucleus; SC, superior colliculus.

1. Lein ES, et al. (2007) Genome-wide atlas of gene expression in the adult mouse brain. *Nature* 445:168–176.
2. Ng L, et al. (2009) An anatomic gene expression atlas of the adult mouse brain. *Nat Neurosci* 12:356–362.
3. Rowell JJ, Mallik AK, Dugas-Ford J, Ragsdale CW (2010) Molecular analysis of neocortical layer structure in the ferret. *J Comp Neurol* 518:3272–3289.

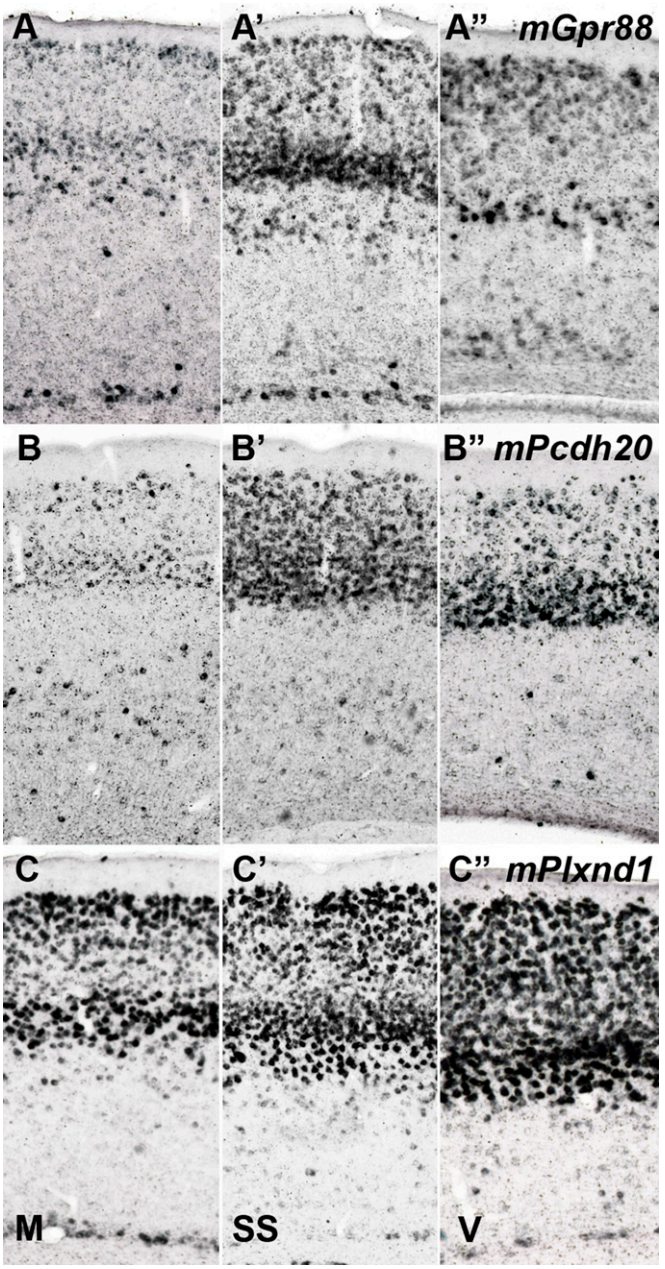

Fig. S2. Molecular examination of additional candidate layer 4 markers in mouse neocortex. In a recent RNAseq study, Belgard et al. (1) characterized gene expression in different layers of adult mouse neocortex by microdissection. We reviewed their top 200 "enriched in layer 4" genes through the CORTx browser (2). The list included the layer 4 markers *Eag2* and *Rorb*, but not *Whrn*. Cross-referencing Belgard et al.'s (1) transcriptomic atlas indicated greater expression in layers 2/3 or in layer 5 than in layer 4 for many of these genes. For promising candidates, we consulted the Allen Brain Atlas (http://www.brain-map.org) and in some cases isolated cDNAs and carried out the ISH in our laboratory. Illustrated are three examples (*Gpr88*, *Pcdh20*, and *Plxnd1*) of the CORTx-identified genes we tested directly. Unfortunately, these searches did not yield additional selective markers of layer 4; the candidate genes were either not differentially enriched in layer 4 or show marked variation across neocortical areas. (*A*–*C*′′) ISH in the mouse for G protein-coupled receptor 88 (*Gpr88*; *A*–*A*′′); protocadherin 20 (*Pcdh20*; *B*–*B*′′); and plexin D1 (*Plxnd1*; *C*–*C*′′) in motor cortex (M; *A*, *B*, and *C*), somatosensory cortex (SS; *A*′, *B*′, and *C*′), and visual cortex (V; *A*′′, *B*′′, and *C*′′). *Gpr88* is expressed in upper layer 5 in M, SS, and V cortex, and is only prominent in layer 4 of SS cortex. *Pcdh20* labeling is strong in layer 4 of V cortex and in layers 2–4 of SS cortex, but is only weakly expressed in M cortex. *Plxnd1* is nowhere restricted to layer 4.

1. Belgard TG, et al. (2011) A transcriptomic atlas of mouse neocortical layers. *Neuron* 71:605–616.
2. Medical Research Council Functional Genomics Unit (2011) CORTx: A Functional Browser for the Transcriptomes of Neocortical Layers. Available at http://genserv.anat.ox.ac.uk/cortx. Accessed September 20, 2011.

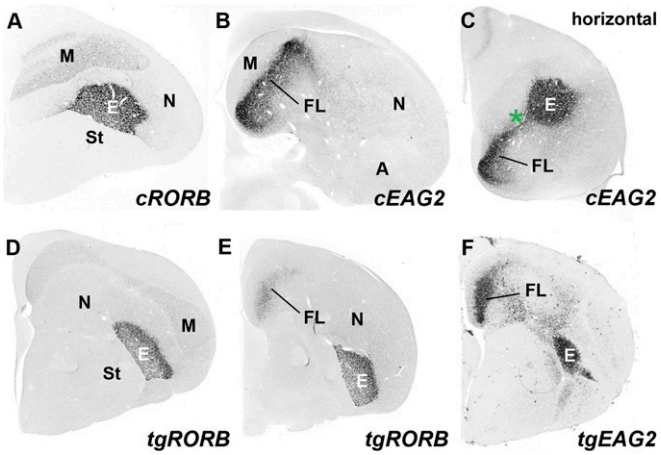

Fig. S3. Molecular identification of layer 4 cell types in the avian DVR. (*A*–*C*) The entopallium and Field L in the chicken express the layer 4 markers *RORB* and *EAG2*. (*A*) Entopallium expression of *RORB*. (*B*) Field L expression of *EAG2*. Coronal cross-sections from anterior (*A*) and posterior (*B*) telencephalon processed for ISH. (*C*) DVR horizontal section demonstrates the tissue bridge between the entopallium and Field L that expresses high levels of *EAG2* (asterisk). Anterior is to the top of the panel. (*D*–*F*) The entopallium and Field L of the zebra finch (*Taeniopygia guttata*) express the layer 4 marker genes *RORB* (*D* and *E*) and *EAG2* (*F*). The basorostral pallial nucleus (1) is the only DVR site apart from the entopallium and Field L that coexpresses *EAG2* and *RORB* transcripts. The basorostral nucleus is the target of ascending somatosensory input from the brainstem (2–4). These projections bypass the dorsal thalamus, directly innervating the telencephalon by the quintofrontal pathway. The basorostral nucleus is therefore not thalamorecipient, but it is equivalent to the entopallium and Field L in being a lemniscal target nucleus in the telencephalon, where "lemniscus" refers to "fiber systems originating from secondary sensory cell groups and ascending toward the forebrain" (5). Gene expression for *RORB* (but not for *EAG2*) is also prominent in the avian mesopallium, with appreciable levels in the chicken mesopallium (*A*) and more moderate levels in zebra finch mesopallium (*D*). Unlike the hyperpallium, the nidopallium, and the arcopallium, there is no circuit evidence that the mesopallium contains layer 4- or layer 5-type cells. A, arcopallium; E, entopallium; FL, Field L; M, mesopallium; N, nidopallium; St, striatum.

1. Reiner A, et al.; Avian Brain Nomenclature Forum (2004) Revised nomenclature for avian telencephalon and some related brainstem nuclei. *J Comp Neurol* 473:377–414.
2. Wild JM, Reinke H, Farabaugh SM (1997) A non-thalamic pathway contributes to a whole body map in the brain of the budgerigar. *Brain Res* 755:137–141.
3. Wild JM, Arends JJ, Zeigler HP (1985) Telencephalic connections of the trigeminal system in the pigeon (*Columba livia*): A trigeminal sensorimotor circuit. *J Comp Neurol* 234:441–464.
4. Wild JM, Farabaugh SM (1996) Organization of afferent and efferent projections of the nucleus basalis prosencephali in a passerine, *Taeniopygia guttata*. *J Comp Neurol* 365:306–328.
5. Nauta WJH, Karten HJ (1970) A general profile of the vertebrate brain, with sidelights on the ancestry of cerebral cortex. *Neurosciences: Second Study Program*, ed Schmitt FO (Rockefeller Univ Press, New York), pp 7–26.

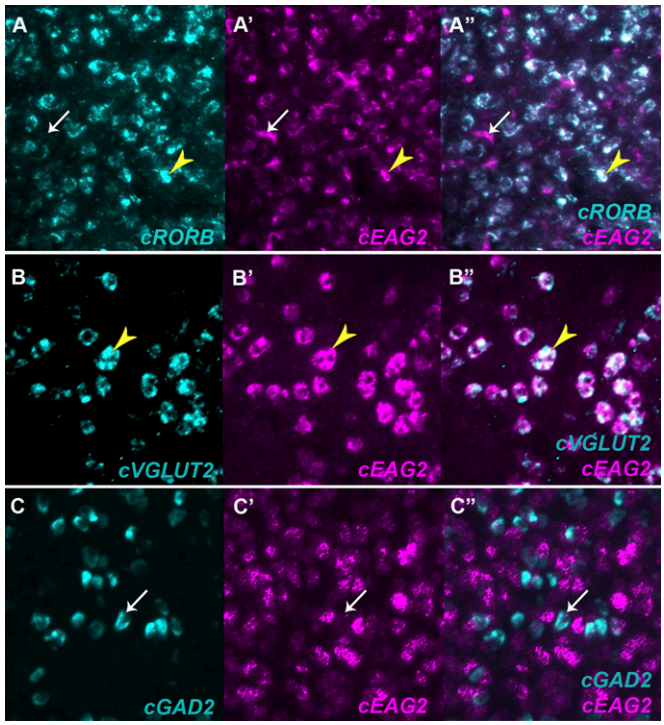

Fig. S4. Molecular characterization of layer 4 cell types in the chicken entopallium. (*A*–*A*′′) Three-panel FISH demonstration of coexpression of the validated layer 4 markers *RORB* and *EAG2* in the chicken entopallium, as documented in the single panel of Fig. 2*F*. (*B*–*B*′′ and *C*–*C*′′) The *EAG2*-rich cells of the entopallium are excitatory. Two-color FISH shows that *EAG2*-positive cells are enriched in mRNA for the vesicular glutamate transporter gene *VGLUT2/SLC17A6* (*B*–*B*′′) and do not express the GABA synthetic enzyme gene *GAD2/GAD65* (*C*–*C*′′). Yellow arrowheads (*A*–*A*′′ and *B*–*B*′′) mark double-labeled cells. White arrows (*A*–*A*′′ and *C*–*C*′′) mark corresponding positions in the photomicrographs, indicating singly labeled cells. Note that not all *EAG2*-rich cells in the entopallium express *RORB* (*A*′ and *A*′′; see main text).

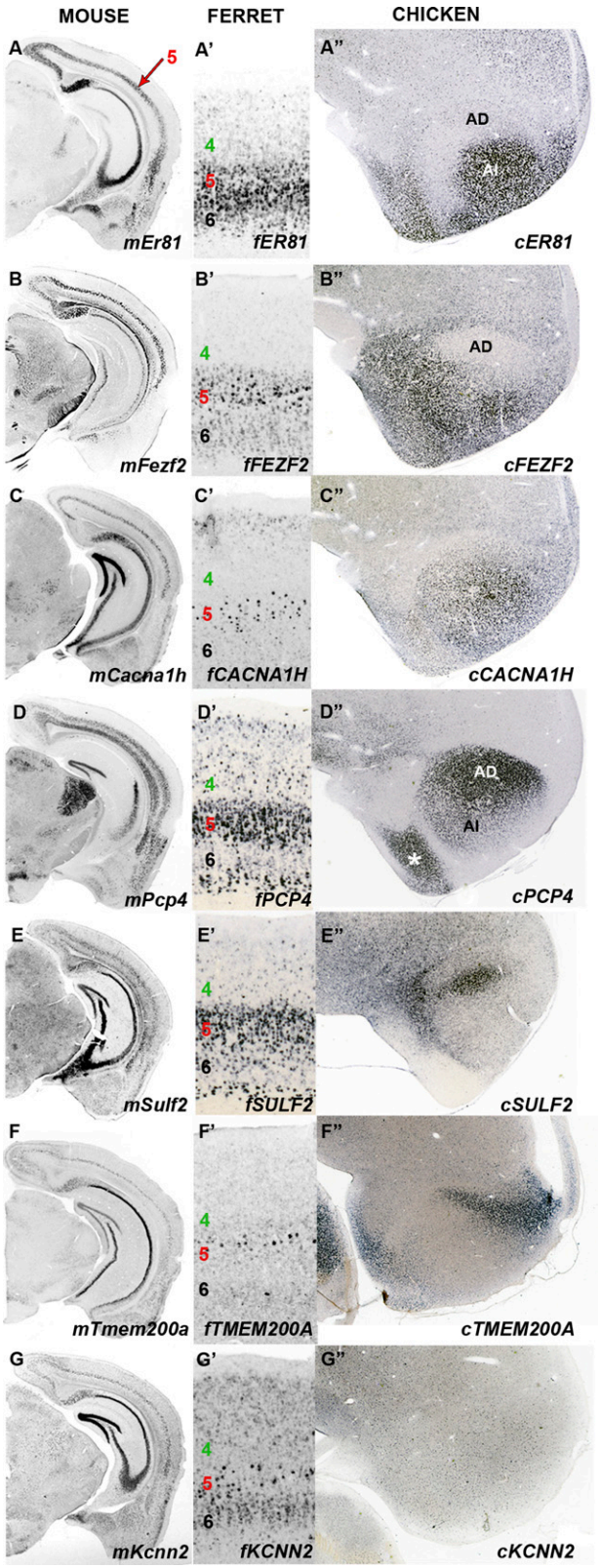

Fig. S5. Molecular characterization of layer 5 markers in the mammalian neocortex and the avian DVR. (*A*–*G*) ISH experiments demonstrating *Er81* (*A*), *Fezf2* (*B*), *Cacna1h* (*C*), *Pcp4* (*D*), *Sulf2* (*E*), *Tmem200a* (*F*), and *Kcnn2* (*G*) gene expression in layer 5 (*A*, red arrow) of mouse neocortex. (*A′*–*G′*) High-power photomicrographs of ferret neocortical area 18 prepared for ISH. All seven mouse layer 5 marker genes are also expressed in ferret layer 5. (*A′′*–*G′′*) High-power photomicrographs of coronal sections from posterior chicken telencephalon demonstrate expression of six of the seven mammalian layer 5 markers in the arcopallium; the exception is *KCNN2* (*G′′*) expression, which was not selectively localized to the arcopallium (see main text). The layer 5 markers in the arcopallium were found in the dorsal arcopallium, the intermediate arcopallium, or both [see labeling in *D′′*, which follows the arcopallium naming conventions recommended by the Avian Brain Nomenclature Forum (1)]. Both the dorsal arcopallium and the intermediate arcopallium have been shown to give rise to

Legend continued on following page

brainstem projections in chickens (2) and other birds (3–5). The subnuclear heterogeneity seen in layer 5 gene expression patterns in the arcopallium is consistent with the sublamina complexity of layer 5 of mammalian neocortex (6) and may reflect differences in brainstem projection targets (4, 5, 7). Some of these layer 5 marker genes are also expressed in the nucleus noted with an asterisk (*D′*). Reiner et al. (figure 8*C* in ref. 1) identified this territory as the posterior pallial amygdala, or PoA. In the pigeon, this PoA territory is reported to have fiber connections similar to those of the mammalian basolateral amygdala and to not project to hindbrain (8). Interestingly, in the mouse, the basolateral nucleus of the amygdala does express some layer 5 markers, including *Er81* (9). 4,5,6, layers 4, 5, and 6 in ferret neocortex; A, arcopallium; AD, dorsal arcopallium; AI, intermediate arcopallium.

1. Reiner A, et al.; Avian Brain Nomenclature Forum (2004) Revised nomenclature for avian telencephalon and some related brainstem nuclei. *J Comp Neurol* 473:377–414.
2. Davies DC, Csillag A, Székely AD, Kabai P (1997) Efferent connections of the domestic chick archistriatum: A phaseolus lectin anterograde tracing study. *J Comp Neurol* 389:679–693.
3. Wild JM, Arends JJ, Zeigler HP (1985) Telencephalic connections of the trigeminal system in the pigeon (*Columba livia*): A trigeminal sensorimotor circuit. *J Comp Neurol* 234:441–464.
4. Wild JM, Farabaugh SM (1996) Organization of afferent and efferent projections of the nucleus basalis prosencephali in a passerine, *Taeniopygia guttata*. *J Comp Neurol* 365:306–328.
5. Bottjer SW, Brady JD, Cribbs B (2000) Connections of a motor cortical region in zebra finches: Relation to pathways for vocal learning. *J Comp Neurol* 420:244–260.
6. Rowell JJ, Mallik AK, Dugas-Ford J, Ragsdale CW (2010) Molecular analysis of neocortical layer structure in the ferret. *J Comp Neurol* 518:3272–3289.
7. Mello CV, Vates GE, Okuhata S, Nottebohm F (1998) Descending auditory pathways in the adult male zebra finch (*Taeniopygia guttata*). *J Comp Neurol* 395:137–160.
8. Atoji Y, Saito S, Wild JM (2006) Fiber connections of the compact division of the posterior pallial amygdala and lateral part of the bed nucleus of the stria terminalis in the pigeon (*Columba livia*). *J Comp Neurol* 499:161–182.
9. Lein ES, et al. (2007) Genome-wide atlas of gene expression in the adult mouse brain. *Nature* 445:168–176.

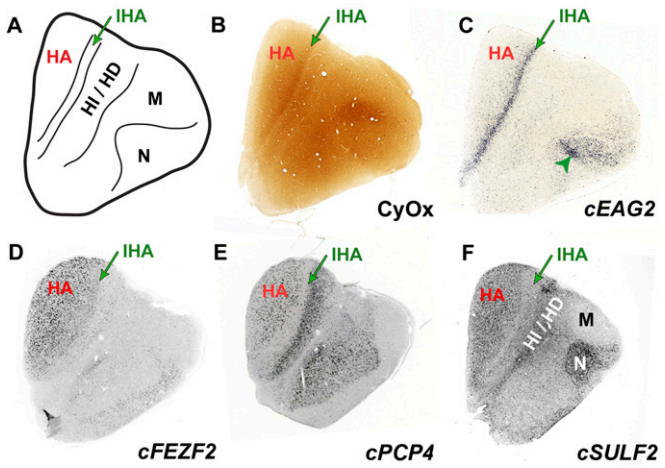

Fig. S6. The Wulst has L4/I and L5/O cell types. (*A*) Diagram of a cross-section through anterior chicken telencephalon illustrating the nuclear organization of the Wulst. The interstitial part of the hyperpallium apicale (IHA; green) is the target of thalamic input and the hyperpallium apicale (HA; red) contains Wulst output neurons projecting to brainstem. (*B* and *C*) The thalamorecipient IHA expresses the L4/I molecular markers. (*B*) The IHA, which is not readily localized in Nissl preparations of chicken brain, was identified with cytochrome oxidase (CyOx) histochemistry. CyOx activity is a general marker for thalamorecipient territories in amniote forebrain; for example, CyOx staining is enriched in thalamorecipient layer 4 of mammalian visual cortex (1), and, in the avian DVR, intense CyOx staining coincides precisely with the distributions of thalamic axons to the entopallium and Field L (2, 3). (*C*) The L4/I marker *EAG2* is expressed as a stripe that precisely aligns (green arrow) with the IHA identified in the serially adjoining section (*B*) stained for CyOx. The green arrowhead notes the anterior tip of the entopallium. (*D–F*) The neurons of the output nucleus HA are enriched in the L5/O marker genes *FEZF2* (*D*), *PCP4* (*E*), and *SULF2* (*F*). The HA is the exclusive source of Wulst projections to the brainstem (4, 5). Some layer 5 markers, such as *PCP4* (*E*) and *SULF2* (*F*), are also expressed in the Wulst nuclei that flank the IHA laterally, that is, in the hyperpallium intercalatum (HI) and the hyperpallium densocellulare (HD). Although the HI and HD do not send axons to the brainstem, they do project to the thalamus (6). In mammals, many layer 5 molecular markers are also expressed in layer 6, which projects to thalamus but not to brainstem (7). M, mesopallium; N, nidopallium.

1. Livingstone MS, Hubel DH (1982) Thalamic inputs to cytochrome oxidase-rich regions in monkey visual cortex. *Proc Natl Acad Sci USA* 79:6098–6101.
2. Wild JM, Karten HJ, Frost BJ (1993) Connections of the auditory forebrain in the pigeon (*Columba livia*). *J Comp Neurol* 337:32–62.
3. Krützfeldt NO, Wild JM (2005) Definition and novel connections of the entopallium in the pigeon (*Columba livia*). *J Comp Neurol* 490:40–56.
4. Reiner A, Karten HJ (1983) The laminar source of efferent projections from the avian Wulst. *Brain Res* 275:349–354.
5. Wild JM, Williams MN (2000) Rostral wulst in passerine birds. I. Origin, course, and terminations of an avian pyramidal tract. *J Comp Neurol* 416:429–450.
6. Korzeniewska E, Güntürkün O (1990) Sensory properties and afferents of the N. dorsolateralis posterior thalami of the pigeon. *J Comp Neurol* 292:457–479.
7. Rowell JJ, Mallik AK, Dugas-Ford J, Ragsdale CW (2010) Molecular analysis of neocortical layer structure in the ferret. *J Comp Neurol* 518:3272–3289.

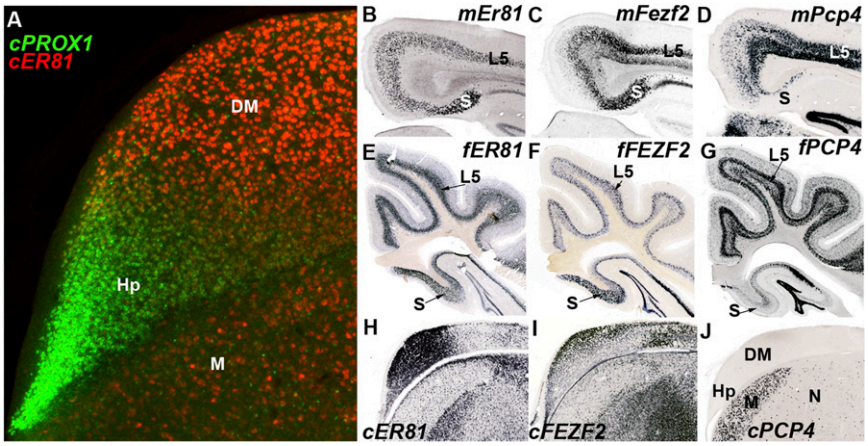

Fig. S7. The chick parahippocampal area does not contain neurons homologous to deep-layer neocortical cells. (*A*) Regional molecular organization of chick medial pallium illustrated by two-color FISH for the dentate gyrus marker *PROX1* (green) and the subiculum marker *ER81* (red). (*B–J*) Coronal sections of mouse (*B–D*) and ferret (*E–G*) dorsomedial telencephalon, stained for the L5/O markers *Er81* (*B* and *E*), *Fezf2* (*C* and *F*), and *Pcp4* (*D* and *G*). *Er81* and *Fezf2* are strongly expressed in the deep layers of neocortex and in the subiculum (S) of the hippocampal formation. *Pcp4* is also enriched in deep layers of the neocortex but is expressed in only a small subpopulation of subicular neurons. (*H–J*) The proposed chick homolog of the subiculum is a dorsomedial (DM) region of the chick parahippocampal area. Gene expression for *ER81* (*H*) and *FEZF2* (*I*) is enriched in DM. *PCP4* (*J*), by contrast, is expressed by only a few DM neurons, which are not visible at this magnification. Hp, hippocampus; L5, layer 5; M, mesopallium; N, nidopallium.

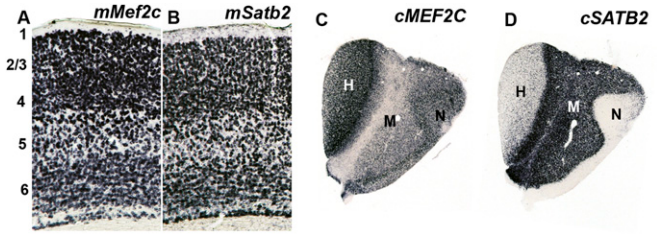

Fig. S8. *Mef2c* and *Satb2* gene expression is not specific to upper layers of the neocortex. *Mef2c* (*A*) and *Satb2* (*B*) are expressed in layers 2–6 of adult mouse neocortex. *MEF2C* (*C*) and *SATB2* (*D*) are widely expressed in the P15 chick dorsal telencephalon, and their patterns are broadly complementary, with *MEF2C* labeling being densest in the hyperpallium (H) and *SATB2* labeling being heaviest in the mesopallium (M). 1–6, layers of neocortex; N, nidopallium.